RSC Advances

ROYAL SOCIETY OF CHEMISTRY

www.rsc.org/advances

A table of contents entry:

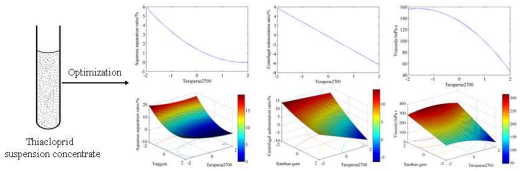

A response surface methodology with four factors at five levels was adopted to optimize a model thiacloprid suspension concentrate.

Cite this: DOI: 10.1039/c0xx00000x

www.rsc.org/xxxxxx

ARTICLE TYPE

Thiacloprid suspension formula optimization by a response surface methodology

Bei-xing Li, Wei-chang Wang, Kai Wang, Da-xia Zhang, Lei Guan and Feng Liu*

Received (in XXX, XXX) Xth XXXXXXXXX 20XX, Accepted Xth XXXXXXXXX 20XX

DOI: 10.1039/b000000x

Abstract: A model thiacloprid 25 % suspension concentrate was prepared using Tersperse2700 (X_1), AE1601 (X_2), xanthan gum (X_3) and veegum (X_4). A response surface methodology (RSM) was used to evaluate the influences of four experimental factors on the aqueous separation ratio (R_1), centrifugal sedimentation ratio (R_2) and viscosity (R_3). The results show that the main factors influencing the three responses were X_3, X_4 and X_2 followed by X_1; moreover, several interactions were also significant. Multiple-response optimization was performed based on a desirability function, considering the minimum R_1, R_2, and R_3 as well as the financial cost. The integrated optimum conditions were X_3 = 0.24 % , X_4 = 1.33 % , X_2 = 0.50 %, and X_1 = 2.90 % (mass fraction). A verification experiment demonstrated that the optimized formula R_1, R_2, and R_3 were 1.69 %, 2.63 % and 257.74 mPa s with the average relative predicted value errors 7.69 %, 4.18 % and -1.41 %, respectively. The response surface methodology is an effective approach for optimizing the suspension concentrate formula with comprehensive advantages.

Keywords: thiacloprid; suspension concentrate; response surface methodology; central composite design; physical stability

Introduction

Suspension is a common form for many products including biomaterial, food, pharmaceutical and paint. Its application in pesticide has also garnered extensive attention. Aqueous suspension concentrate (SC) is one of the most widely used types of pesticide formulation, especially for pesticides with poor water-solubility and a relatively high melting point[1]. Rapid SC development is closely related to such unique advantages. Water is the primary medium, not an organic solvent, in a topical SC formula, in contrast to an emulsion concentrate formula, which tends to decrease its environmental and financial costs. In addition, the small SC particle size enhances the biological activity of the active ingredient[2]. However, as the particle size decreases, the specific surface area and surface energy significantly increase, which produces flocculation or agglomeration[3]. Therefore, a formula with balanced properties is necessary to reduce flocculation, agglomeration and the sedimentation caused by gravitational stress[1]. The triangular diagram and orthogonal design methods are often used to simplify the optimization procedure. Orthogonal design is a classic fractional design method widely used in many domains with specially designed experiment tables[4-6]; in the triangle-coordinate method, several representative points on the triangle are selected[7, 8]. Both methods can optimize the procedure and formula, where only several factors are considered. However, the SC was composed of multiple components (often more than four) that it is difficult to use the triangular diagram and orthogonal design methods to determine the precise effect of each component if the interactions are considered[9, 10].

Among experimental designs, the response surface methodology (RSM) is the most effective method for improving and optimizing experimental procedures using a series of statistical and mathematical techniques[11-13]. It is especially appropriate for analyzing and modeling multi-factor experiments because it can assess both the single and interaction effects for specific factors. In recent years, the RSM has significantly advanced in the food industry, pharmaceuticals, chemical engineering, architecture, energy sources and other fields[14-19]. However, few researchers have reported on the RSM in pesticide formulations mainly because its statistics and analyses are complicated. Thiacloprid, which is a type of neuroactive chemical modeled after nicotine, is a second neonicotinoid insecticide[20]. It was first developed by Bayer Crop Science and launched under the brand name Calypso[21]. Thiacloprid is highly efficient at controlling sucking insects and chewing insects, including aphids, jassids, whiteflies, mites and weevils[22, 23]. The technical material of thiacloprid describes crystals at room temperature with a white to light brown color. It includes a 136 °C melting point, relatively low water solubility (only 184 mg l^{-1}) and excellent chemical stability in water; thus, it is appropriate for constructing SC products[1, 24].

As proof, a model thiacloprid SC was prepared to investigate the influence of wetting-dispersing agents and anti-settling agents on sample properties using the RSM. The physical stability, viscosity, fluidity, dispersibility, size distribution and

suspensibility of the samples were measured. The strategy adopted for obtaining an optimized formula is expected to provide practical information to advance pesticide formulations.

Results and discussion

The design matrix for the proposed experiments and their corresponding output parameters are shown in Table S1 (Supplementary Information). The 27 samples exhibited favorable fluidity and dispersibility. In addition, the suspensibility of the samples before storage was measured from 92.84 % to 97.02 %, which did not affect the applied performance of the suspension concentrate; thus, the suspensibility was not further optimized. The high suspensibility cannot be separated from the relationship between the small particle size and high-efficient dispersant. The sedimentation or floating of dispersing particles in the diluent must individually obey Stokes' law to a certain extent. As the density of the thiacloprid technical material is greater than the disperse phase, the particles sediment in the diluents, and the settling rate positively correlates with the square of the particle size. Therefore, the settling rate was slow for the 27 samples, wherein the particles were smaller than 3 μm. The average particle diameter of the 27 samples ranged from 1.51 μm to 2.50μm. However, it should be noted that Ostwald ripening was obviously observed for most samples, especially after hot storage. Thiacloprid includes 184 mg l^{-1} water solubility at 20 °C; however, it is more soluble in water with an increase in temperature. In addition, an accelerated test was conducted at 54 ± 2 °C; thus, the thermal motion of the particles was greatly accelerated, which also aggravated the Ostwald ripening. Fortunately, the suspensibility of all samples remained greater than 91 %, even after hot storage (Table S1, Supplementary Information). The aqueous separation ratios (R_1) of the tested samples ranged from 1 % to 17 %, and the centrifugal sedimentation ratio (R_2) ranged from 2 % to 23 %. A similar variance trend was observed for R_1 and R_2, but the variance trend for viscosity was somewhat discrepant. We expected to generate a preparation with R_1 and R_2 values lower than 5 %; the moderate viscosity (R_3) was welcome. Therefore, the data for the three dependent variables were analyzed to obtain a formula that meets the above criteria.

Optimizing the aqueous separation ratio

Table 1 Fitness of the aqueous separation ratio to different models.

Model	Sequential *p*-value	Lack of fit *p*-value	Adjusted R^2	Predicted R^2
Linear	< 0.0001	0.0073	0.7648	0.7137
2FI[a]	0.0899	0.0095	0.8251	0.8256
Quadratic polynomial	< 0.0001	0.1951	0.9925	0.9807
Cubic polynomial	0.2484	0.2201	0.9957	0.9251

[a] 2FI: the two-factor interaction model

A regression analysis was performed to fit the R_1 results using the Design-expert software. Linear, 2FI, quadratic and cubic polynomial equations were used to test the fitness (Table 1). The data showed that higher "Adjusted R^2" and "Predicted R^2" values yielded a better fit. As shown in Table 1, both the quadratic and cubic polynomial models showed favorable fitness with "Adjusted R^2" and "Predicted R^2" values greater than 0.9. The *p*-value is an index that indicates the significance of the data, which essentially yields a "Prob > *F*" value. The sequential *p*-values for the linear and quadratic polynomial models were below 0.05, which indicates significant models. The lack of fit *p*-value indicates whether the "lack of fit" is significant relative to the pure error. The data show that the linear and 2FI models could not fit the R_1 data; the lack of fit *p*-values were below 0.05. Considering the four evaluation indexes, the polynomial model best fit the data; therefore, it was used to indicate the adequacy of the fitted model. The quadratic polynomial model is described as follows[25, 26].

$$Y = b_0 + \sum_{i=1}^{4} b_i \times X_i + \sum_{i=1}^{4} b_{i,j} \times X_i \times X_j + \sum_{i=1}^{4} b_{i,i} \times X_i^2 \quad (1)$$

Y is the dependent variable, b_0 is the intercept, the X_i terms are the independent variables, and the b_i, $b_{i,j}$, $b_{i,i}$ terms are the relative coefficients. Previous publications show that the polynomial model best fits the experimental data when interactions between the independent variables are significant[27]. The suspension concentrate is the type of complicated formulation for which interactions between different adjuvants are inevitable.

An analysis of variance (ANOVA) was then performed based on Fischer tests, and the corresponding *p*-value is listed in Table S2 (Supplementary Information) with the regression equation coefficients. The *F* value is a statistical parameter of the Fischer test that indicates whether the data deviates from the mean as well as the relevance between the proposed model and experimental results. The model *F*-value R_1 was 248.39, which implies a significant model with only a 0.01 % chance that a "Model *F*-value" this large could be produced from noise. Table S2 shows that X_1, X_2, X_3, X_4 and seven other terms significantly influenced R_1. The $p > 0.05$ indicates that the model terms were not significant. In this case, reducing the model by removing the model terms with sequential *p* values greater than 0.05 was the best way to improve the model[14]. The prediction equation for R_1 (coded value) is described as follows.

$$\text{Aqueous separation ratio (\%)} = 3.35 - 1.17X_1 - 1.56X_2 - 2.43X_3 - 2.62X_4 - 0.235X_1X_4 + 1.29X_2X_3 + 1.04X_3X_4 + 0.391X_1^2 + 0.679X_2^2 + 0.834X_3^2 + 1.49X_4^2 \quad (2)$$

X_1, X_2, X_3 and X_4 in equation 2 are Tersperse2700, AE1601, xanthan gum and veegum, respectively.

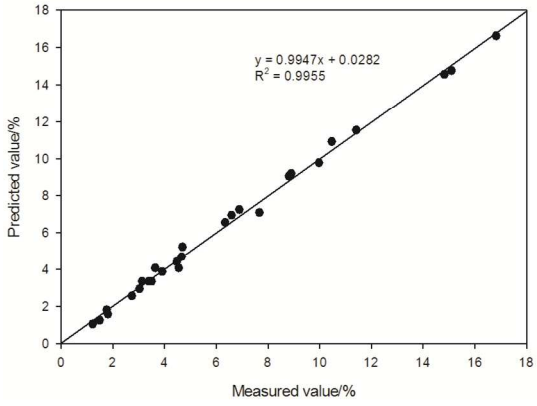

Fig. 1 Measured values vs. predicted values for modeled aqueous separation ratio.

The absolute value of the regression coefficients reflects the influence of each term on the responses; the positive and negative sign demonstrates that both high and low levels of the terms considered are approximately optimal.The predicted values for R_1 were generated after calculating the coded value using equation 2. The predicted values and observed values were then regressed, as depicted in Figure 1. The empirical equation fits well to the data and yields a R^2 = 0.9955 (Coefficient of determination). As shown in Table 2, the optimal conditions for R_1 were generated by analyzing equation 3 using the "fmincon function" in MATLAB R2014a, and the minimal R_1 was estimated at -0.03 %. Although the R_1 was favorable, the actual mass fractions of Tersperse2700 and AE1601 were slightly high, which is not economical.

Table 2 The optimal conditions for the aqueous separation ratio.

Factor	Level	Actual mass fraction/%
X_1: Tersperse2700	1.92	2.96
X_2: AE1601	2.00	2.50
X_3:Xanthan gum	-0.94	0.18
X_4: Veegum	1.36	1.68

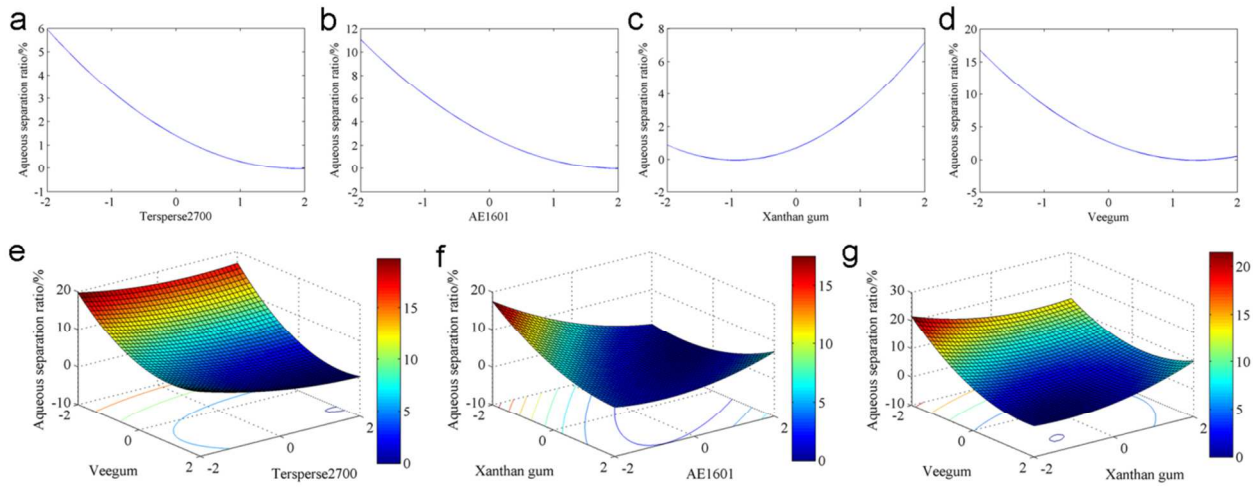

Fig. 2 The response surface plots for aqueous separation ratio.

Response surface plots can effectively indicate interactions between dependent variables and aid in generating optimal responses with balanced conditions. With R_1 as the response, the response surface plots are shown in Figure 2. Significant decreases in R_1 were observed with increasing levels of Tersperse2700, AE1601 and veegum (Figure 2a, 2b and 2d); the three other variables remained at the optimal levels. However, when their levels reached 1.0, R_1 only changed slightly. The influence of xanthan gum differed greatly, as depicted in Figure 2c. When the level of xanthan gum was low, R_1 decreased slightly; however, at high levels of xanthan gum, R_1 increased significantly with the level of xanthan gum. Based on the above analysis, we conclude that maintaining the three variables at optimal levels and the latter variable at a moderate level yields a qualified thiacloprid 25% SC. The interactions between Tersperse2700 and veegum, AE1601 and xanthan gum, and xanthan gum and veegum significantly influenced R_1 when the two other variables remained at their optimal levels (Figure 2e, 2f and 2g). The R_1 decreased abruptly with variations in the veegum level when the Tersperse2700 level changed; fortunately, when the veegum quantity was maintained at the highest level, R_1 was lower than 5% (Figure 2e). As shown in Figure 2f, R_1 was lower than 5% when either AE1601 or xanthan gum was at its highest level. When xanthan gum was at a low level, the R_1 decreased more or less. However, when high levels of xanthan gum were added, the phenomena differed greatly. A slight increase in R_1 was observed when the veegum level varied from 0 to 2 (coded value).

Centrifugal sedimentation ratio optimization

The centrifugal sedimentation ratio (R_2) regression analysis results are shown in Table S3 (Supplementary Information). The four models exhibited "Adjusted R^{2}" and "Predicted R^{2}" values greater than 0.95, which implies favorable fitness. However, a sequential $p > 0.05$ was observed for the cubic polynomial model, which indicates insignificant models; however, the linear, 2FI and quadratic polynomial models were all significant models. The lack of fit p-values for the linear and 2FI models were lower than 0.05, which indicates a large experimental error. Therefore, the polynomial model was the best model for fitting the R_2 results. An ANOVA was used to indicate the adequacy of the fitted polynomial model; the results are shown in Table S4 (Supplementary Information). The model F-value was 940.72, which indicates a favorable explanation of the adopted model. Considering the p-values of the factors in Table S4, X_1, X_2, X_3, X_4, X_1X_3, X_2X_3, X_3X_4, X_2^2, X_3^2 and X_4^2 are all significant model terms for R_2. The model terms with sequential p-values higher than 0.05 were removed to improve the predicted model, which yielded the following empirical equation:

$$\text{Centrifugal sedimentation ratio } (\%) = 11.6 - 1.83X_1 - 2.43X_2 - 3.65X_3 - 2.39X_4 - 0.589X_1X_3 + 0.483X_2X_3 - 0.294X_3X_4 + 0.153X_2^2 + 0.324X_3^2 + 0.605X_4^2 \quad (3)$$

The predicted R_2 values were generated after calculating the coded values using equation 3. The predicted R_2 values were then regressed using the observed values, as illustrated in Figure S1 (Supplementary Information). The empirical equation fit well to the experimental data (R^2 = 0.9987). Using equation 3, we deduced that R_2 decreased with the mass fraction of the four

adjuvants. Furthermore, the minimum was estimated at -6.30 % when the adjuvant doses reached the highest level. R_2 cannot be negative. In this case, the emphasis on generating the lowest R_2 through maintaining the variables at their highest level was a wasted effort.

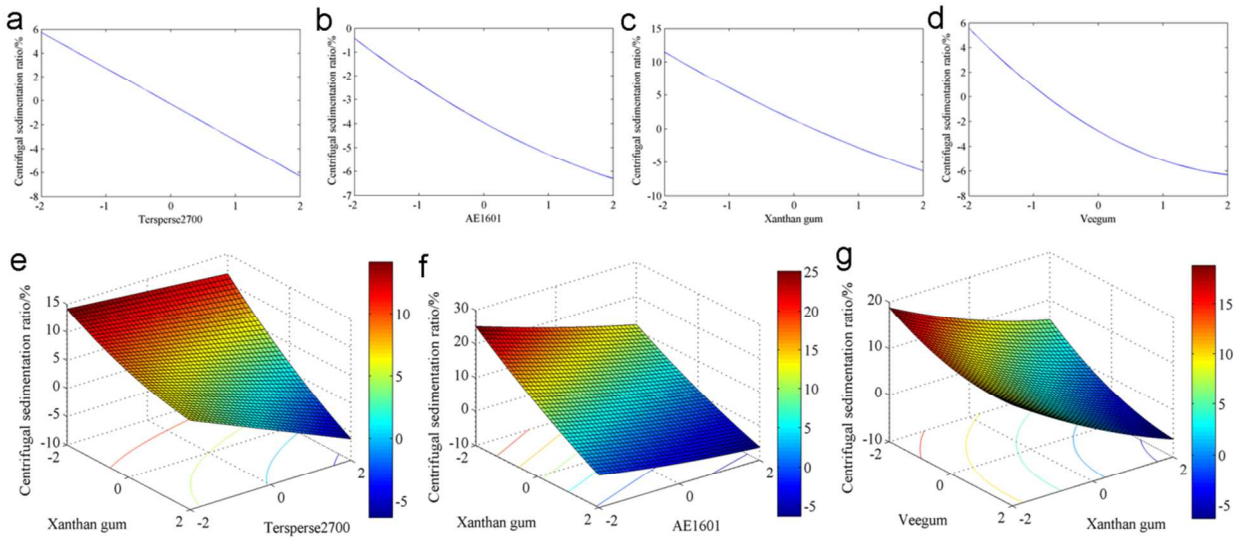

Fig.3 The response surface plots for centrifugal sedimentation ratio.

To clearly investigate the influence of four factors on R_2, the response surfaces were plotted. First, three variables were maintained at their optimal levels, and the other variable ranged from -2.0 to 2.0 (coded value) to discern the influence of a certain variable. As illustrated in Figure 3a, significant decreased were observed for R_2 with increasing levels of Tersperse2700. The singular influences form AE1601, xanthan gum or veegum exhibited the same trend, as depicted in Figure 3b, 3c and 3d. However, as indicated from equation 3, the optimal levels of the three constant variables were the highest levels. Furthermore, maintaining the latter variable at a high level would cause equipment damage because this experiment would be performed at the extreme conditions. The interactions between Tersperse2700 and xanthan gum, AE1601 and xanthan gum, xanthan gum and veegum exhibited significant influences on R_2. As depicted in Figure 3f, the R_2 decreased significantly with the AE1601 and xanthan gum levels when the other two variables were maintained at an optimal level (also the highest level, 2.0). A similar trend was observed for the interactions between Tersperse2700 and xanthan gum (Figure 3e) as well as xanthan gum and veegum (Figure 3g).

Viscosity optimization

The viscosity regression analysis results are shown in Table S5(Supplementary Information). The cubic polynomial model yielded a sequential *p*-value greater than 0.05, which implies that the model is insignificant. Furthermore, the linear model could not fit the viscosity results based on a significant "Lack of fit". Both the 2FI and quadratic polynomial models were appropriate for fitting the viscosity results. However, the quadratic polynomial model exhibited a lower "Lack of fit"; therefore, it was more suitable for fitting the viscosity results.

The ANOVA was used to indicate the adequacy of the fitted polynomial model; the results are shown in Table S6 (Supplementary Information). The model *F*-value was 112.04, which indicates a significant model with only a 0.01 % chance that a "Model *F*-value" this large could be due to noise. Based on the sequential *p*-values in Table S5, X_2, X_3, X_4, X_1X_2, X_1X_3, X_2X_4, X_3X_4 and X_1^2 are significant model terms for viscosity. The model terms with sequential $p > 0.05$ were removed to improve the predicted model, which yielded the following empirical equation.

$$\text{Viscosity (mPa} \cdot \text{s)} = 254 + 21.3X_2 + 37.6X_3 + 24.3X_4 + 7.76X_1X_2 + 5.86X_1X_3 + 9.01X_2X_4 + 3.55X_3X_4 - 8.36X_1^2 \quad (4)$$

The predicted viscosity values were obtained after calculating the coded value using equation 4. Next, the predicted and observed values were regressed, as shown in Figure S2 (Supplementary Information). The empirical equation fit well to the data (R^2 = 0.9841). The minimal viscosity could be estimated using the "fmincon function" of MATLAB R2014a. Using equation 4, the optimal conditions for minimal viscosity are determined as X_1 = 2.00, X_2 = -2.00, X_3 = -2.00 and X_4 = 2.00, and the minimum was estimated at 47.05 mPa s. However, the optimal conditions for minimal viscosity were inconsistent with favorable physical stability. Next, the response surfaces were plotted to discern the influence of the independent variables on viscosity.

When the Tersperse2700 was low, the viscosity of the preparation changed slightly. However, the viscosity decreased abruptly when the Tersperse2700 amount exceeded 0 (Figure 4a). A significant increase of the viscosity was observed with an increase in either the AE1601 or xanthan gum level, as illustrated in Figure 4b and 4c. Although the viscosity decreased significantly with the veegum level, only a slight decrease in viscosity was observed (Figure 4d). For the significant interactions, a similar trend in viscosity variations was observed for the interactions between Tersperse2700 and AE1601 (Figure 4e) as well as Tersperse2700 and xanthan gum (Figure 4f). The viscosity increased abruptly with the AE1601 level regardless of the Tersperse2700 quantity added, as shown in Figure 4e. The

Tersperse2700 influence differed greatly. When AE1601 was maintained at the lowest level, the viscosity decreased more or less with an increasing level of Tersperse2700. However, opposite results were observed when AE1601 was maintained at its highest level (Figure 4f). The veegum quantity barely influenced the viscosity when the AE1601 was maintained at a low level; however, the viscosity significantly increased with the veegum level when high levels of AE1601 were added (Figure 4g). As illustrated in Figure 4h, a significant change in viscosity was not observed with varying levels veegum regardless of the xanthan gum quantity applied. However, the viscosity increased in an approximately linear manner with the xanthan level. Thus, we conclude that maintaining Tersperse2700 at a high level as well as maintaining AE1601 and xanthan gum at low levels is highly beneficial for producing SC samples with low viscosity, but the veegum level is not important.

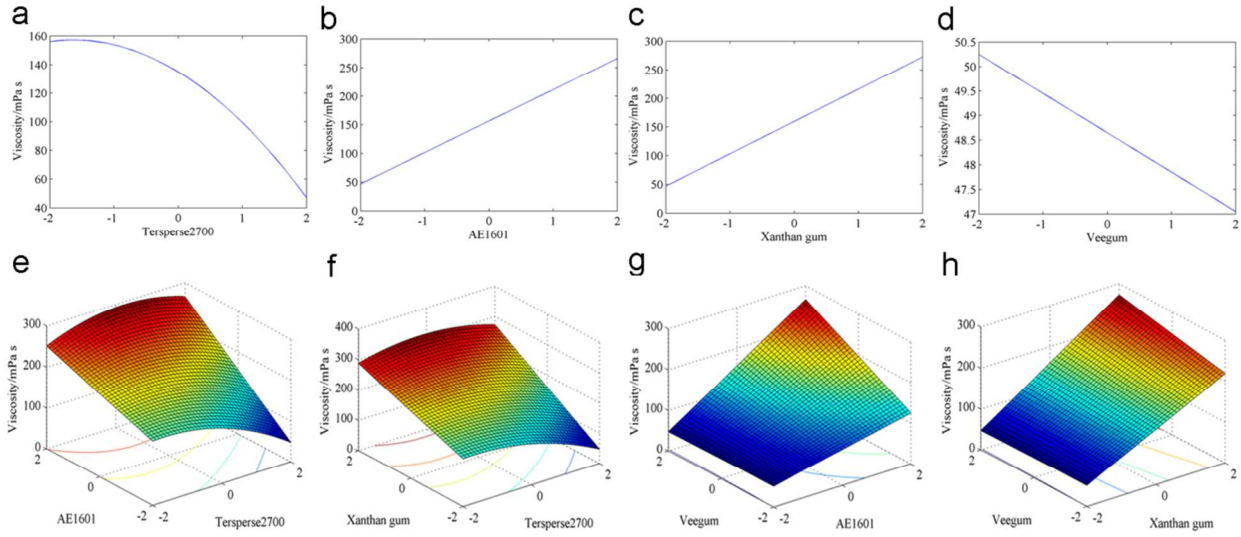

Fig.4 The response surface plots for viscosity.

Multiple-response optimization

The most important goal for applying RSM is process optimization. Herein, the three individual responses were the aqueous separation ratio, centrifugal sedimentation ratio and viscosity. However, minimum optimizations were generated under different conditions. To optimize the parameters using the three output responses, a compromise among the conditions for different responses is desirable. The notion of a desirability function was employed, for which the total desirability was determined as a geometric mean of the individual desirability functions[28, 29]. To determine the optimal conditions, the desirability function was fit using the least-squares model. Generally, a qualified SC product should include an aqueous separation ratio lower than 5 % and centrifugal sedimentation ratio lower than 5 %. The viscosity is relevant to fluidity and dispersibility of a preparation, and high viscosity often yields poor fluidity and dispersibility. Fortunately, the sample viscosity ranged from 160.34 mPa s to 345.78 mPa s. Because the viscosity was not concerning, it was considered a less important response during the optimization process. The optimized conditions were derived by minimizing the above three responses; the constraints are shown in Table S7 (Supplementary Information). The level of variability that yielded the highest desirability (> 0.90) was then used as the optimum level. Twenty-four solutions were generated when only the preparation formula was considered. However, we also expected to use as little dispersant as possible due to financial constraints. Therefore, the integrated optimum of variables were X_1 = 1.80, X_2 = -1.99, X_3 = 1.84 and X_4 = 0.66; namely, the true mass fractions of each component were 2.90 % Tersperse2700, 0.50 % AE1601, 0.24 % xanthan gum and 1.33 % veegum, respectively. The predicted values calculated using equation (2), (3) and (4) were 1.82 % (R_1), 2.74 % (R_2) and 254.11 mPa s (R_3), respectively. The SC sample prepared under optimal conditions was also produced and tested. The measured sample values for R_1, R_2 and R_3 were 1.69 % ± 0.18 %, 2.63 % ± 0.27 % and 257.74 ± 0.35 mPa s (mean ± SE). The average relative errors of the predicted values above were 7.69 %, 4.18 % and -1.41 %, respectively. As shown above, the desirability function introduced herein exhibited favorable effectiveness at multiple-response optimization. However, it should be noted that the fitness of the applied regression model decreased with the imported dependent variables. It was better to remove the unimportant indexes in the formulation before the multiple-response optimization.

Experimental

Materials

Thiacloprid (purity > 95 %) was purchased from Shandong Sino-Agri United Biotechnology Co., Ltd. (Shandong, China) to prepare the SC. Agricultural emulsifier No. 1601 (AE1601) was purchased from the Jiangsu Hai'an Petrochemical Plant (Jiangsu, China), and Tersperse2700 (polycarboxylate, M_w = 7808), which is a type of high-efficiency dispersant, was provided by Huntsman (Salt Lake City, USA). Xanthan gum (purchased from Deosen Biochemical Ltd., Shandong, China) and magnesium aluminum silicate (Veegum, provided by Sinoma Mineral Materials Company, Jiangsu, China) were used to adjust the viscosity of the preparation and are known as anti-settling agents.

SC preparation

AE1601 is a segmented copolymer with the structure EO-PO-EO (Ethylene oxide - Propylene epoxide - Ethylene oxide), which yields favorable wettability and, thus, plays a role as a wetting agent[30]. Tersperse2700 is a comb-polymer with high levels of carboxyl in its molecular structure, which produce effective charge repulsion[31]. Furthermore, it can be adsorbed on the particle surface and exhibit favorable steric hindrance[31]. Their chemical structure are shown as Scheme 1 and Scheme 2, respectively. It should be noted that both AE1601 and Tersperse2700 can provide wetting or dispersing functions; therefore, they were used as the investigated factors herein. Xanthan gum is a polysaccharide with a distinctive anti-settling specialty and is commonly used in SC due to its shear thinning property[32]. Shear thinning indicates that the SC will be high-viscous upon standing and very thin after applying stress or strain, which is a significant advantage for liquid preparations. Previous articles demonstrate that physical stability can be significantly meliorated through combining magnesium aluminum silicate and xanthan gum mainly due to a synergistic effect[33]; thus, magnesium aluminum silicate was also used as an anti-settling agent. The typical procedure used herein is as follows. Wet grinding was performed to generate thiacloprid 25 % SC, and the grinding conditions were then determined. First, 52.63 g thiacloprid technical material, a certain weight of wetting-suspending agents and anti-settling agents, 4 g glycerol and 1 g defoamer were accurately weighed, and distilled water was used to complement 200 g. Next, the mixture was added to a stainless steel cup with 200 ml zirconium oxide beads. Finally, the samples were ground at 1700 r/min for 1 h to generate a homogeneous thiacloprid 25 % SC. Cooling water was used throughout the grinding process to maintain a relatively stable temperature around the container.

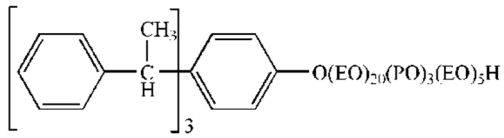

Scheme 1 Chemical structure of AE1601.

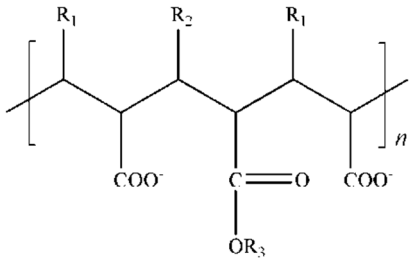

Scheme 2 Chemical structure of Tersperse2700 (R_1, R_2 and R_3 are simple hydrophobic groups)

Response surface methodology experiment

The RSM is a useful model for clarifying how multiple variables influence the responses in a complicated but effective manner based on the experimental design[34-38]. Among the second-order RSM designs, the Box-Behnken design and central composite design (CCD) are the most frequently used designs[39-41]. The CCD is a five-level experimental design, and the Box-Behnken design is a three-level design; thus, the accuracy of the CCD experiments may be better. An additional advantage to CCD is that it can be used to avoid continued experimentation at extreme conditions. Such conditions are often difficult to generate or control; thus, they may increase the potential for equipment damage[11]. The CCD experiments were designed by Design Expert 8.05 (Stat-Ease Inc., Minneapolis, USA) with four factors at five levels. Both the factors and levels were derived from the literature[42]. The data analyses and model building were also performed using the same software. To prepare thiacloprid SC, wetting-suspending agents and anti-settling agents were added in accordance with Table 3.

Table 3 Factors and levels of RSM experiment.

Factor(mass fraction)	Level				
	-2	-1	0	1	2
X_1: Tersperse2700/%	1.00	1.50	2.00	2.50	3.00
X_2: AE1601/%	0.50	1.00	1.50	2.00	2.50
X_3: Xanthan gum/%	0.16	0.18	0.20	0.22	0.24
X_4: Veegum/%	0.00	0.50	1.00	1.50	2.00

Measuring quality control indexes

In principle, two types of accelerated experiments were performed to assess the physical stability of SC. In the first accelerated experiment, we measured thermal physical stability. First, 16 g of the prepared sample was accurately weighed using an analytical balance (± 0.0001 g, Sartorius, Goettingen, Germany); it was then sealed in a 20-ml tube with a stopper. Next, the tube was transferred to an oven for 14 d at a constant temperature (54 ± 2 °C). To enhance the experimental precision, the measurements were repeated in triplicate. Aqueous separation after hot storage was used to evaluate the advantages to thermal physical stability as shown in equation 5.

$$\text{Aqueous separation ratio}\ (\%) = \frac{m_{up}}{m_{to}} \times 100 \qquad (5)$$

m_{up} and m_{to} are the weight of separated aqueous phase after hot storage and the total weight of the sealed sample, respectively. The data demonstrate that more aqueous separation yields worse physical stability. The second accelerated test included measuring the centrifugal stability. An 8 g sample was accurately weighed and sealed in a 10-ml centrifuge tube. The sample was then centrifuged at 3000 r/min for 30 min in a high-speed refrigerated centrifuge (Hitachi, Tokyo, Japan). After centrifugation, the centrifuge tube was inverted for 60 s to remove the upper suspension, and the residual substance at the bottom was regarded as sediment. The centrifugal sedimentation ratio was defined as the ratio of the sediment weight to the total weight of the sample. The experiment was repeated for each preparation, and the data were presented as the mean ± SE (standard error). A lower centrifugal sedimentation ratio indicates better physical stability.

A laser particle size analyzer (Zhuhai OMEC instrument Co., Ltd., Guangdong, China) was used to evaluate the thiacloprid SC size distribution. It was measured four times, and the median diameter (D_{50}) was the selected parameter. Most pesticide SC products are composed of pseudoplastic fluid, wherein the apparent viscosity decreases with the shear rate, which is shear thinning[43]. A rheometer (Brookfield, Massachusetts, USA) in a

thermostatic bath (25 °C) was used, and the samples were measured at a 10 s^{-1} shear rate through reading viscosity values every 20 s based on a previously reported method[44]. The sample dispersibility and suspensibility measurements were performed using the methods recommended by the Collaborative International Pesticides Analytical Council (CIPAC), namely CIPAC MT160 and CIPAC MT184, respectively.

Conclusion

The main factors that influenced the aqueous separation ratio (R_1), centrifugal sedimentation ratio (R_2) and viscosity (R_3) were xanthan gum (X_3), veegum (X_4) and AE1601 (X_2) followed by Tersperse2700 (X_1); in addition, several interactions were significant. The optimal conditions were mainly based on the minimum R_1, R_2, and R_3; and financial cost was determined. The integrated optimum conditions were $X_3 = 1.84$, $X_4 = 0.66$, $X_2 = -1.99$ and $X_1 = 1.80$; namely, the true mass fractions for each component were 0.24 %, 1.33 %, 0.50 % and 2.90 %, respectively. The optimum conditions yielded R_1, R_2, and R_3 values at 1.69 % ± 0.18 %, 2.63 % ± 0.27 % and 257.74 ± 0.35 mPa s (mean ± SE) with the average relative predicted value errors being 7.69 %, 4.18 % and -1.41 %, respectively. The RSM is an effective approach for optimizing the suspension concentrate formula; moreover, it can promote comprehensive advantages by properly adjusting the levels of several adjuvants based on practical requirements.

Acknowledgement

The authors gratefully acknowledge Ms. Wei Mu from Shandong Agricultural University for her helpful suggestions for this manuscript. This work was supported by a grant from the Special Fund for Agro-scientific Research in the Public Interest from the Ministry of Agriculture of China (201303027).

Notes and references

Key Laboratory of Pesticide Toxicology & Application Technique, Shandong Agricultural University, Tai'an, P. R. China. Fax/Tel: 86 0538 8242611; E-mail: fliu@sdau.edu.cn

The authors declare no competing financial interest.

† Electronic Supplementary Information (ESI) available: [The design matrix for the proposed experiments and their corresponding output parameters are shown in Table S1. The regression equation coefficients and ANOVA for the aqueous separation ratio (Table S2), centrifugal sedimentation ratio (Table S4) and viscosity (Table S6) are listed as supplementary information. The fitness of centrifugal sedimentation ratio results to different models is listed as Table S3, and that for viscosity is displayed in Table S5. Moreover, the constraints for the multiple-response optimization are shown in Table S7. Figure S1 and Figure S2 which illustrated the measured values vs. predicted values for modeled centrifugal sedimentation ratio and viscosity are also listed as supplementary information]. See DOI: 10.1039/b000000x/

1. M. A. Faers and G. R. Kneebone, *Pestic Sci*, 1999, **55**, 312-325.
2. S. Haas, H.-W. Hässlin and C. Schlatter, *Colloids Surf A*, 2001, **183–185**, 785-793.
3. H. Li, F. Lu, H. Wang, L. Zhai and X. Li, *Chin J Appl Chem* 2012, **29**, 327-331.
4. C. Díez, E. Barrado, P. Marinero and M. Sanz, *J Chromatogr A*, 2008, **1180**, 10-23.
5. Z. Wang and H. Wang, *Chin J Aeronaut*, 2012, **25**, 887-895.
6. J. Luo, G. Zhu, F. Zhang, Q. Li, T. Zhao and X. Zhu, *RSC Adv*, 2015, **5**, 6071-6078.
7. E. Helm and B. Trolle, *Wallerstein Lab Commun*, 1946, **9**, 181-191.
8. C. Ma, F. Liu, W. Mu, Z.-r. Han and Z.-l. Chen, *Chin J Pestic Sci*, 2006, **8**, 379-382.
9. D.-x. Zhang, F. Liu, G.-s. Zhang, B. Chen and X.-n. Yang, *Sci Agric Sin*, 2011, **44**, 2469-2475.
10. G. Taguchi and M. S. Phadke, in *Quality Control, Robust Design, and the Taguchi Method*, ed. K. Dehnad, Springer US, 1989, pp. 77-96.
11. E. McCarthy, S. Flick and W. Mérida, *J Power Sources*, 2013, **239**, 399-408.
12. J.-p. Zhang, X.-l. Hou, T. Yu, Y. Li and H.-y. Dong, *J Integr Agric*, 2012, **11**, 151-158.
13. G. E. P. Box and K. B. Wilson, *J Roy Stat Soc B* , 1951, **13**, 1-45.
14. W. Arbia, L. Adour, A. Amrane and H. Lounici, *Food Hydrocolloids*, 2013, **31**, 392-403.
15. K.-N. Chen, M.-J. Chen and C.-W. Lin, *J Food Eng*, 2006, **76**, 313-320.
16. M. Aghbashlo, H. Mobli, S. Rafiee and A. Madadlou, *Powder Technol*, 2012, **225**, 107-117.
17. J.-P. Wang, Y.-Z. Chen, Y. Wang, S.-J. Yuan and H.-Q. Yu, *Water Res*, 2011, **45**, 5633-5640.
18. M. O. Hamzah, B. Golchin and C. T. Tye, *Constr Build Mater*, 2013, **47**, 1328-1336.
19. L. Xin, X. Jinyu and L. Weimin, *RSC Adv*, 2015, **5**, 1598-1604.
20. N. J. Bostanian, J. M. Hardman, H. A. Thistlewood and G. Racette, *Pest Management Science*, 2010, **66**, 1263-1267.
21. A. Elbert, M. Haas, B. Springer, W. Thielert and R. Nauen, *Pest Manag Sci*, 2008, **64**, 1099-1105.
22. S. Dong, K. Qiao, H. Wang, Y. Zhu, X. Xia and K. Wang, *Pest Manag Sci*, 2014, **70**, 1267-1273.
23. S. Dong, K. Qiao, Y. Zhu, H. Wang, X. Xia and K. Wang, *Crop Prot*, 2014, **58**, 1-5.
24. T. NAKAMURA, H. SHIMIZU, M. FUJIMOTO, Y. TAKAHI and Y. KONDO, *J Pestic Sci*, 1981, **6**, 293-300.
25. J. Liu, F. Chen, W. Tian, Y. Ma, J. Li and G. Zhao, *J Agric Food Chem*, 2014, **62**, 7532-7540.
26. G. Peretto, W.-X. Du, R. J. Avena-Bustillos, J. D. J. Berrios, P. Sambo and T. H. McHugh, *J Agric Food Chem*, 2014, **62**, 984-990.
27. M. Ghadiri, S. Fatemi, A. Vatanara, D. Doroud, A. R. Najafabadi, M. Darabi and A. A. Rahimi, *Int J Pharm*, 2012, **424**, 128-137.
28. Z. He, P.-F. Zhu and S.-H. Park, *Eur J Oper Res*, 2012, **221**, 241-247.
29. H. Heidari and H. Razmi, *Talanta*, 2012, **99**, 13-21.
30. X.-g. Zhang, J.-x. Liu, H.-y. Wang, M.-y. Wang and Z.-j. Fan, *Acta Phys-Chim Sin*, 2010, **26**, 617-625.
31. C. Ma, Y. Xu, X.-y. Guo, X.-r. Luo and X.-m. Wu, *Chem J Chin Univ*, 2013, **34**, 1441-1449.
32. D. Pooja, S. Panyaram, H. Kulhari, S. S. Rachamalla and R. Sistla, *Carbohydr Polym*, 2014, **110**, 1-9.
33. B. Li, K. Wang, D. Zhang, C. Zhang, L. Guan and F. Liu, *Chin J Pestic Sci*, 2013, **15**, 692-698.
34. V. B. Silva and A. Rouboa, *Appl Math Comput*, 2012, **218**, 6733-6743.

35. F. Tabandeh, M. Khodabandeh, B. Yakhchali, H. Habib-Ghomi and P. Shariati, *Chem Eng Sci*, 2008, **63**, 2477-2483.
36. M. Aghbashlo, H. Mobli, A. Madadlou and S. Rafiee, *J Microencapsul*, 2012, **29**, 790-804.
37. S. Mayengbam, H. Yang, V. Barthet, M. Aliani and J. D. House, *J Agric Food Chem*, 2013, **62**, 419-426.
38. B. S. Kaith, R. Sharma, S. Kalia and M. S. Bhatti, *RSC Adv*, 2014, **4**, 40339-40344.
39. V. Hosseinpour, M. Kazemeini and A. Mohammadrezaee, *Chem Eng Sci*, 2011, **66**, 4798-4806.
40. N. Şahín, C. C. Akoh and A. s. Karaalí, *J Agric Food Chem*, 2006, **54**, 3717-3722.
41. E. Pourbasheer, S. Sadafi, M. R. Ganjali and M. Abbasghorbani, *RSC Adv*, 2014, **4**, 62190-62196.
42. B. Li, W. Wang, D. Zhang, K. Wang, L. Guan and F. Liu, *Sci Agric Sin*, 2015, **48**, 280-292.
43. J. Shen, Q.-l. Huang, J.-b. Xia, D. Chen, D.-m. She, F.-m. Li and W. Hu, *Chin J Pestic Sci*, 2008, **10**, 354-360.
44. L.-f. Li, L. Wang, J.-w. Wang and D.-q. Wang, *Acta Chim Sin*, 2011, **69**, 1760-1764.